

TWELFTH EUROPEAN ROTORCRAFT FORUM

Paper No. 83

SUBSTANTIATION OF THE ANALYTICAL PREDICTION  
OF GROUND AND AIR RESONANCE STABILITY OF A  
BEARINGLESS ROTOR, USING MODEL SCALE TESTS

P.T.W.Juggins

Westland plc, Helicopter Division

Yeovil, England

September 22 - 25, 1986

Garmisch-Partenkirchen  
Federal Republic of Germany

Deutsche Gesellschaft für Luft- und Raumfahrt e. V. (DGLR)  
Godesberger Allee 70, D-5300 Bonn 2, F.R.G.

SUBSTANTIATION OF THE ANALYTICAL PREDICTION  
OF GROUND AND AIR RESONANCE STABILITY OF A  
BEARINGLESS ROTOR, USING MODEL SCALE TESTS

P.T.W.Juggins  
Westland PLC Helicopter Division  
Yeovil, England

ABSTRACT

Prediction of the ground and air resonance stability of a bearingless main rotor demands the use of analytical techniques which adequately address the particular characteristics associated with this type of rotor.

The approach adopted in such an analytical procedure is described and the substantiation of analysis by testing of a scale model bearingless main rotor is reported.

Substantiation is achieved, from generally good agreement between measured and theoretical data, although parameters are identified which hindered clear evaluation of some stability margins by the Moving Block technique.

The effects of pitch-lag coupling on stability are discussed, from measured results and from a theoretical study.

Implications for added damping requirements on a full scale rotor are identified.

1. INTRODUCTION

A design feasibility study of bearingless main rotors has recently been performed at Westland. A part of that study has been the assessment of ground and air resonance stability margins of such rotors in combination with existing and projected airframe configurations, using predictive analyses.

Such evaluation of the stability characteristics of a bearingless rotor requires the appropriate formulation and application of analytical tools, so that any properties of this type of rotor are fully accounted for. Properties likely to be encountered include the existence of multiple load paths of significant flexibility and length in the mechanism of pitch application, the possibility of significant warping effects and shear deformation in a hub flexure element, and the likely existence of high levels of coupling between blade pitch and flap motions and between blade pitch and lag motions.

The approach taken at Westland has been to calculate the natural frequencies and mode shapes of a rotating single blade and hub arm of bearingless configuration, and then use the modes as degrees of freedom in subsequent stability analyses. A computer program has been developed to predict the natural frequencies and mode shapes of a multiple load-path rotor (which are also used in predictions of rotor response and loads). Calculated modes have then been used to predict ground and air resonance stability in an analysis which utilises the predominant components of

fundamental flap and lag mode shapes together with pitch-flap and pitch-lag coupling coefficients.

The need to substantiate these predictive analyses by comparison with experimental data was addressed by ground and air resonance tests in still air of a model bearingless main rotor, which were performed at EEL Limited, Cowes, finishing in August 1985. Existing test rigs and rotor blades were used, together with model bearingless rotor hubs. In the theoretical predictions, wherever possible each stage of the analytical process was checked against available measurements, but measured values were not adopted in subsequent stages. In this way a substantiation of the complete predictive method was sought.

## 2. PREDICTION METHODS

### 2.1 Bearingless Rotor Modes Analysis

This analysis has the facility to model twin hub flexure elements, one of which may be a torque-tube or enveloping torque-sleeve used in application of pitch to the blade. Each load path is reduced to a beam model with cross-sectional properties defined at up to 10 points on each flexure and 40 points on the blade. There is a general description of geometry, by specifying end co-ordinates for the flexures and for up to 23 straight blade segments, to enable the analysis of swept tips. Control system attachment via a torque-tube or torque-sleeve may be specified with a point spring to earth (in 6 degrees of freedom) at the root of the second flexure to model a shear restraint. There is a stiffness and inertia model for the control circuit.

The equations of motion are solved by application of a transfer matrix technique with compatibility conditions at the junction of the twin hub flexures and the blade. Six displacement degrees of freedom are defined at up to 200 points on each flexure and 700 points on the blade. Non-linear equations are solved iteratively to define the steady state conditions, with an applied aerodynamic load distribution. The natural frequencies and normal mode shapes are calculated as a perturbatory solution about the steady state.

The equations of motion, which include the ability to describe transverse shear as well as axial, torsion and bending flexibility, were formulated using the application of Hamilton's Principle to strain energy, kinetic energy and virtual work expressions. The derivation has some similarities with the work in Reference 1, and with the Westland analysis used for semi-rigid and articulated rotors. The effect of warping restraint in the hub flexures is described by applying, to the cross-section torsional stiffness distribution, factors which are found from a solution of the third-order differential equation in torsion. Previous substantiations have included comparisons with theory for tapered and uniform cantilever beams, comparisons with another analysis in application to semi-rigid rotors, and comparisons with reported measured frequencies for the Boeing Vertol BMR (Reference 2).

## 2.2 Ground and Air Resonance Stability Analysis

This analysis incorporates as degrees of freedom the predominant components of the fundamental flap and lag modes for each blade (flap motion and lag motion, respectively) as well as three translations plus pitch and roll rotations of the fuselage. The fuselage is modelled by five rigid body modes, which may include the effect of connection to earth by springs and dampers. Control laws relating the blade pitch to fuselage angular displacements and rates may be included. Blade pitch motion is not an independent degree of freedom, but is prescribed by the control laws and by specified pitch-flap and pitch-lag coupling coefficients. For the bearingless rotor, these coefficients were defined from the ratio of blade pitch to slope in the fundamental flap and lag modes at 70% rotor radius.

The aerodynamic forcing terms are calculated using quasi-steady aerodynamics, with reverse flow, compressibility and all unsteady effects being ignored. The induced velocity is calculated using momentum theory, and is assumed to be uniform over the entire rotor disc.

The equations of motion describe small perturbations about an equilibrium position; this includes the steady coning angle, cyclic flapping and a uniform aircraft velocity. The blades are not assumed necessarily to be identical.

The program incorporates a facility to calculate the proportions of the blade stiffness, in both the flap and lag modes, due to structural and centrifugal effects. By assuming the mode shapes do not change as rotor speed is varied, the total stiffness at any rotor speed can then be calculated, based on modes defined at a datum speed. The frequency can thus be found, and will only be in error due to the change in strain energy distribution resulting from the change in mode shape. This error is very small, for a wide range of rotor speed. The use of a datum set of modes has the effect of giving a large saving in the computation time required to re-calculate modes at each rotor speed. However, when high levels of pitch-flap and pitch-lag couplings are found in the bearingless rotor, it is important that a single set of modes is not used for too wide a speed range, as couplings are not invariant with rotor speed.

Previous substantiation of the analysis has come from both model scale and full scale test results for semi-rigid rotor systems.

## 2.3 Fixed-Hub Analysis

Checks of predicted fixed-hub stability of the model bearingless rotor were made prior to running, using a Westland coupled modes stability analysis.

### 3. DESCRIPTION OF TEST MODELS

#### 3.1 The Bearingless Model Rotor

The model rotor used existing blades which had previously been used in scale model ground and air resonance tests of a semi-rigid rotor. These were of section NACA 0015, mass balanced to the quarter-chord. The hub was based on a full-size design scheme for a five-bladed main rotor, but a four-bladed configuration was adopted for the model, in order to utilise as many existing components as possible.

The hub flexure element was of multiple-H cross-section, tapered in both flatwise and edgewise dimensions. For the model, a straight taper was adopted in order to simplify manufacture at small scale, while the full-scale scheme included a curved taper. After testing of material specimens, a low (10%) volume-fraction unidirectional GRP material was found to have the correct characteristics and flexure elements were manufactured using a combined process of moulding, machining and finishing by hand. Elements were tested in a fatigue test rig under estimated representative loads, to demonstrate a satisfactory life. Successive specimens were modified until an adequate life was obtained.

The arrangement of the model rotor hub is shown in Figure 1. The flexure elements were attached to a central light alloy hub, with their outer ends fitted to blade root sockets. Alongside each flexure element was a steel torque-tube which was used to transmit pitch to the blades through a universal joint attached to a leading-edge extension of the blade root socket. At its inboard end, the torque-tube was located, with freedom to rotate, in the centre of a steel support flexure connected to the central hub. The steel support flexure provided vertical and lateral shear support, while having a low resistance to motion in the axial direction and to rotational misalignments. The pitch horn was attached to the inner end of the torque-tube and consisted of a plate with alternative attachment holes for the pitch control rod end. Use of the alternative holes enabled control rod inclination to be varied through  $\pm 15$  deg. about an axis parallel to the blade chord line, resulting in changes to pitch-lag coupling.

An earlier torque-tube configuration, based in concept on full-scale schemes, incorporated elastomeric damping discs within a sliding tube, with a ball joint at the inner end. Plain bearings could be substituted for the elastomeric discs. It was found that the inherent damping in this configuration, with or without the elastomeric discs, was too high to allow satisfactory measurement of the rotor stability margins. Consequently the steel support flexure with non-sliding tube was developed to minimise inherent damping.

The central hub and blade root sockets were designed so that a 12 deg. nose-up pre-twist could be applied to the blade either at the flexure element to hub joint or at the flexure element to blade joint. A built-in pre-cone of 2 deg. was included in the hub.

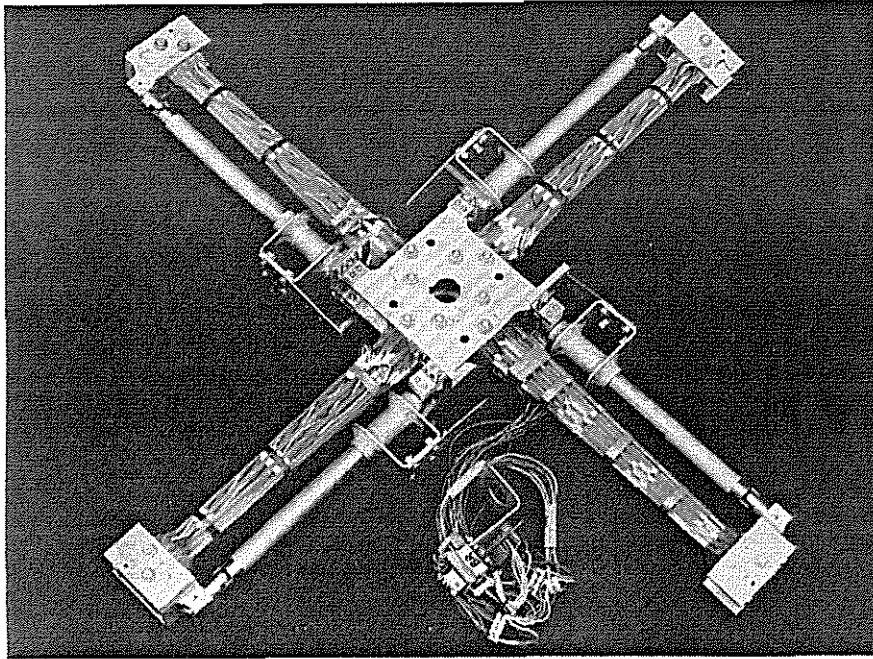


FIGURE 1

Bearingless  
rotor hub

FIGURE 2 Ground resonance model

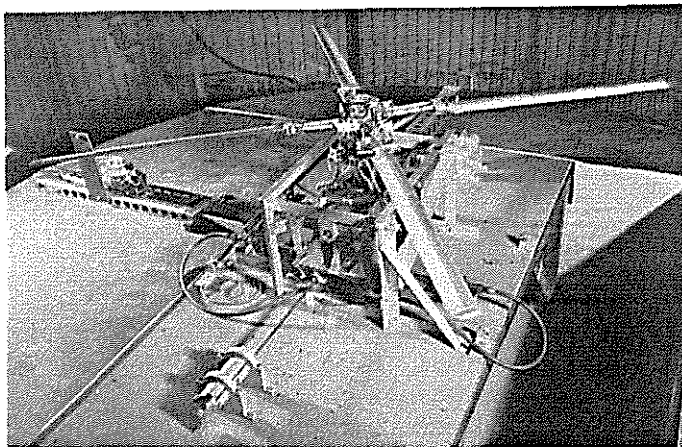
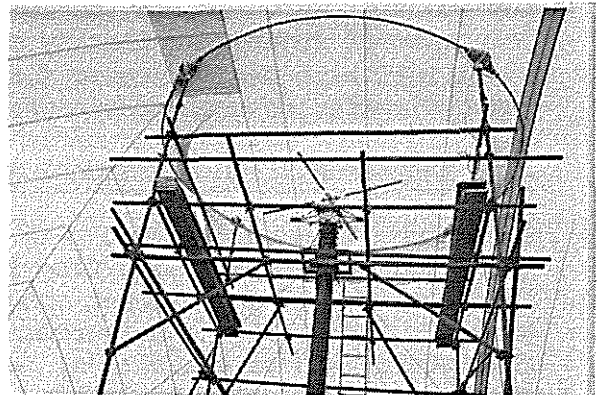


FIGURE 3

Air Resonance test rig



### 3.2 Ground Resonance Rig (Figure 2)

The ground resonance rig had previously been used in studies of a semi-rigid rotor (Reference 3). A scale model fuselage was suspended from an external framework in two fore and aft mounted bearings which gave freedom in roll motion. The roll motion was restrained by cantilever springs of variable length, and hence of adjustable stiffness. The model was mounted on a ground-plane plinth (to simulate ground-effect) and could be locked or released in roll by operation of pneumatic locking pins. Excitation of the fuselage in roll was provided by a remotely-controlled pull-and-release mechanism.

On this model there was no facility to alter blade pitch whilst running the rotor, and testing was performed at constant values of collective pitch. Twelve degrees of pre-twist was incorporated at the flexure element to blade root joint.

### 3.3 Air Resonance Rig (Figure 3)

This rig had also been used in the previous studies (Reference 4). The air resonance model was mounted on a tower, in order to be clear of ground effect, and the fuselage was gimballed to have freedom in both pitch and roll. The previous studies showed that a gimballed model has very similar air resonance characteristics to a fully free model (Reference 4). A lock-down system similar to that of the ground resonance rig was employed, and the drive system flexibility was arranged to give natural frequencies in pitch and roll below 0.7 Hz, in a released state with the rotor stationary.

Cyclic pitch control servos were employed to enable cyclic control while the rotor was running, with collective pitch adjusted only in a stationary condition. Excitation of the fuselage roll and pitch motions was achieved through initiating large excursions by operating the cyclic pitch control. Twelve degrees of blade pre-twist was incorporated at the hub to flexure element joint.

### 3.4 Scaling

The basis of substantiation by test adopted was that of substantiation of predictive methods rather than of a specific rotor design. It was important for this purpose that significant features of a bearingless main rotor were included in the test models. Overall scaling of the models was also required. Hence the models were scaled to one sixth of full size, by the principle of dynamic similarity of Froude and Lock Numbers, based on a full size design scheme for a bearingless main rotor. The rotor diameter of both models was 2.0 metres.

### 3.5 Instrumentation and Signal Analysis

Each hub flexure element was provided with strain gauges measuring the lagwise and flapwise bending responses as well as the torsion of the element about its longitudinal axis. These gauges facilitated measurement of non-rotating vibration characteristics of all blades. When running, measurements were confined to one reference blade.

The most important signal for monitoring was that from the lagwise gauge at the element tip, where the highest measured strain levels were seen. The signal from this gauge was used in the analysis of rotor stability margins.

The model fuselage motions in roll and pitch (air resonance only) were measured by linear displacement transducers, and rotor speed and azimuth position were derived from a magnetic pulse generator.

Measurements were recorded on magnetic tape, and selected samples were analysed on a mini computer, applying the Moving Block technique for estimation of the damping in a decaying signal.

#### 4. TEST PROCEDURES

Before commencing ground or air resonance testing it was necessary to measure vibration characteristics of the individual blades and the fuselage models. Blades were tested in a non-rotating hub-clamped configuration, while the fuselage models were tested with dummy rotor-masses in position. Measurement of response to a deflection and release enabled inherent damping levels and damped natural frequencies to be established. The measured fuselage frequencies and damping were used in the subsequent stability predictions, as were the blade damping levels. Blade frequencies could be compared with calculated values.

The method of test for ground or air resonance consisted of running the rotor to the desired speed, at a pre-set value of collective pitch, releasing the fuselage locking mechanism and recording the flexure element lag strain response to an input disturbance, before locking the fuselage again. In the case of the ground resonance rig, the disturbance was provided by the roll trip mechanism, while for the air resonance rig it was from appropriate application of cyclic pitch.

Stability margins were estimated using application of the Moving Block technique to the decaying lag signal. This technique, described in Reference 5, evaluates the Discrete Fourier Transform of a block of sample points of the signal. The transform is applied at a frequency of interest identified from the spectrum produced by Fast Fourier Transform of the entire signal. If the block of sample points is moved point-by-point through the signal, the damping estimate can be calculated from the approximate slope of a plot of the logarithm of the DFT against block starting time.

The accuracy of this method can be shown to be sensitive to a number of parameters, including frequency resolution, total signal length, block size, windowing methods, the magnitude of initial disturbance relative to the background signal, and the choice of manual or automatic fitting of the straight-line slope. Evaluation of the significance of these various parameters was made during the course of this project. Parameters of particular importance were identified to be frequency resolution limitations when the lag response frequency was close to rotor-speed, and magnitude of initial disturbance.

The stability margins were obtained from the Moving Block analysis in terms of percentage critical damping with respect to the measured lag frequency in the rotating frame of reference.

#### 5. MEASUREMENTS FOR NON-ROTATING BLADE

Figure 4 shows the measured non-rotating blade natural frequencies and damping obtained from decaying oscillation of the ground and air resonance rotors. Corresponding predicted frequencies from the modes analysis are included and show that agreement is good in lag (to within about two percent of the mean

FIGURE 4 BLADE FREQUENCIES & DAMPING NON-ROTATING

NON-ROTATING GROUND RESONANCE ROTOR					NON-ROTATING AIR RESONANCE ROTOR						
BLADE	A	B	C	D	J146*	BLADE	1	2	3	4	J146*
LAG FREQ. (Hz)	7.82	7.95	7.80	7.88	7.75	LAG FREQ. (Hz)	7.91	8.04	7.93	7.94	7.77
DAMPING (%)	1.66	2.53	3.55	1.03	—	Damping (%)	1.65	1.26	1.60	1.50	—
FLAP FREQ. (Hz)	3.85	4.18	4.08	3.91	4.10	FLAP FREQ. (Hz)	3.96	4.06	3.96	3.96	4.11
DAMPING (%)	1.96	3.05	3.85	2.96	—	DAMPING (%)	1.65	1.58	1.41	3.40	—
TORSION FREQ. (Hz)	26.60	27.05	23.83	23.53	22.37	TORSION FREQ. (Hz)	21.00	25.2	25.2	20.50	22.24
DAMPING (%)	9.5	13.0	8.2	10.5	—	DAMPING (%)	18.00	20.1	20.1	9.50	—
(CONTROL ROD DISCONNECTED)					* PREDICTION	(CONTROL ROD DISCONNECTED)					

FIGURE 5 PREDICTED BLADE MODES

**GROUND RESONANCE ROTOR**

ROTOR RPM (= Ω)	COLLECTIVE PITCH (deg.)	LAG FREQ. (Ω)	FLAP FREQ. (Ω)	TORSION FREQ. (Ω)	PITCH-LAG COUPLING CL70*	PITCH-FLAP COUPLING CF70*
900	9	0.686	1.126	3.581	0.015	-0.076
700	9	0.805	1.151	5.420	0.021	-0.041
900**	9	0.686	1.126	—	-0.352	-0.070

\* DEFINED IN SECTION 6

\*\* -15° CONTROL ROD ANGLE

**AIR RESONANCE ROTOR**

ROTOR RPM (= Ω)	COLLECTIVE PITCH (deg.)	LAG FREQ. (Ω)	FLAP FREQ. (Ω)	TORSION FREQ. (Ω)	PITCH-LAG COUPLING CL70*	PITCH-FLAP COUPLING CF70*
900	12	0.678	1.128	1.900	-0.580	-0.622
900	9	0.679	1.130	1.896	-0.216	-0.598
900	6	0.680	1.130	1.892	0.119	-0.550
600	12	0.884	1.183	2.691	-0.549	-0.387
600	9	0.884	1.184	2.688	-0.148	-0.281
600	6	0.885	1.185	2.685	0.217	-0.169

measured value) and flap (to within about three percent), less so in torsion (to within about ten percent). However, it can be noted that differences between mean measurements and theory are less than those between measurements for individual blades. Some large differences in measured damping levels between blades may be attributed to variations introduced by the manufacturing process for the flexure elements. Mean damping measurements were used for the theoretical inherent modal damping in stability predictions, apart from one ground resonance case for which individual blade values were used.

Theoretical frequency predictions for the two rotors are different because of the effects of flexure element pre-twist.

6. PREDICTED ROTATING MODES

Figure 5 shows the predicted fundamental blade mode frequencies for both the ground and the air resonance rotors. Included are values of pitch-lag and pitch-flap couplings, designated CL70 and CF70 respectively.

CL70 is defined as the predicted ratio of blade elastic twist (positive nose-up) to lag slope (positive forward) at 70% rotor radius, in the coupled mode shape identified as fundamental lead-lag.

CF70 is defined as the predicted ratio of blade elastic twist (positive nose-up) to flap slope (positive upward) at 70% rotor radius, in the coupled mode shape identified as fundamental flap.

For the ground resonance rotor it can be seen that coupling magnitudes are low with a vertical control rod. Variation in couplings between the 700 and 900 rpm cases is also low. The flap and lag frequencies, couplings and shapes for the 900 rpm, 9 deg. collective pitch cases were used in subsequent stability predictions. The inclined control rod configuration gave high negative pitch-lag coupling, as was intended.

For the air resonance rotor, frequencies and couplings are shown for 6 deg., 9 deg. and 12 deg. of collective pitch, at 600 and 900 rpm. In stability predictions, the 600 rpm modes were used in the range 400 to 750 rpm and the 900 rpm modes in the range 750 to 1100 rpm. Large magnitudes of pitch-flap and pitch-lag couplings are apparent for the air resonance rotor. Pitch-lag coupling is attributable to the action of steady coning angles producing blade pitch due to lag moments resolved into pitching moments in the deflected hub flexure element. Large resultant modal pitch deflections arise from the low stiffness of the control circuit. Pitch-flap coupling arises from the interaction of the torque-tube geometry and its root spring stiffness with the soft control circuit.

A measured value of 1.75 N/mm was used for the stiffness of the control circuit of the air resonance rotor. This is the stiffness seen in the direction of the control rod (vertical) axis in an asymmetric loading of the control system. The equivalent figure for the ground resonance rotor was 21.0 N/mm, the difference being caused by the inclusion of cyclic pitch control servos on the air resonance rig.

Particularly large variations of pitch-lag coupling with collective pitch were predicted for the air resonance rotor. These suggest that accuracy in the definition of steady lift distributions used in the modes predictions was important.

FIGURE 6

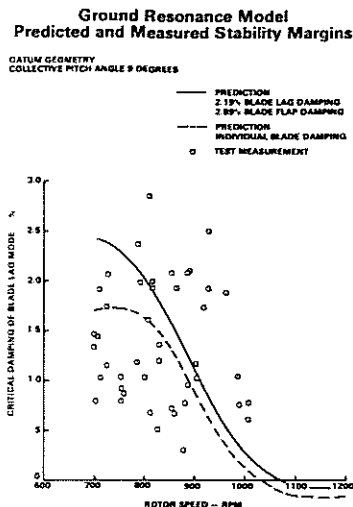
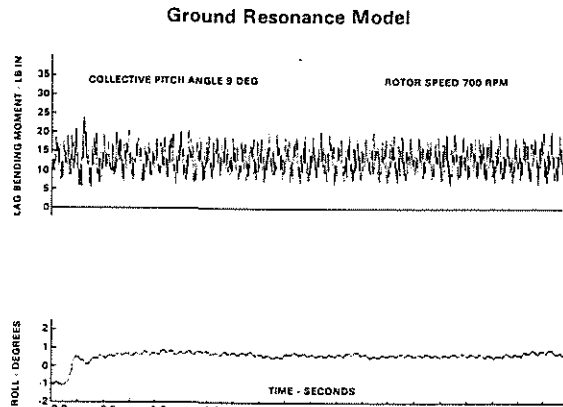


FIGURE 7



## 7. GROUND RESONANCE RESULTS

### 7.1 Nine Degrees Collective Pitch Case

The lag damping estimates obtained from the ground resonance tests for this case are plotted in Figure 6 as points together with a solid line showing theoretical predictions obtained assuming mean inherent blade damping of 2.19 % (lag) and 2.89 % (flap) of critical. The dashed line shows the prediction for an asymmetric rotor with individual inherent blade damping levels as given in Figure 4. The results show that the rotor was stable in the speed range tested, that most measured values are within a band  $\pm 1\%$  either side of the predicted lines, but that scatter of result points at each speed is as high as 1.5% of critical damping.

The most likely reason for the large scatter of results can be seen when an example of the lag signal is studied, shown in Figure 7. The initial disturbance is clearly small in relation to the background signal. The magnitude of disturbance was limited by the available travel in the fuselage roll mechanism, while the magnitude of the background signal was high. The blade-to-blade dissimilarities may have contributed to this, and may have introduced ambiguity in the signal, as suggested in Reference 6. Note that there was no cyclic pitch control to trim out once-per-rev. effects, although individual blade tracking had been set by adjusting control rod length.

Figure 8 shows the variation with rotor speed of predicted roll and regressing lag mode frequencies (seen in the non-rotating frame of reference). Also plotted are measured lag frequency values.

The coalescence of modes which results in the predicted instability above 1000 rpm can be seen. The roll mode frequency increases with rotor speed, from 3.54Hz at zero rpm to 6.85Hz at 1200 rpm. This stiffening can be attributed to coupling with the flapping motion of the blades, in a manner corresponding to the mechanism which generates a non-zero roll frequency in air resonance.

The measured values again show scatter, and suggest that the predictions of lag frequency are low, by about 0.5Hz. This is also seen in Figure 4 for the stationary rotor, suggesting a difference between actual and assumed cross-sectional properties. However, these small frequency differences (less than 5%) have been shown to have little influence on the prediction of the stability margin in this case.

Ground Resonance Model  
Predicted and Measured Freq. for Roll &  
Regressing Lag Modes

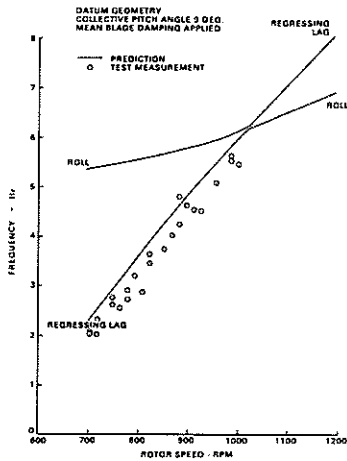


FIGURE 8

Ground Resonance Model  
Predicted and Measured Stability Margins

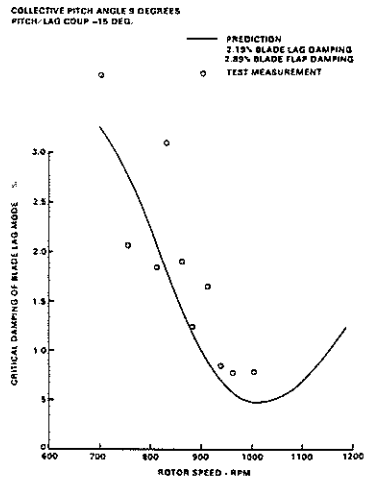


FIGURE 9

Ground Resonance Model  
Predicted and Measured Stability Margins

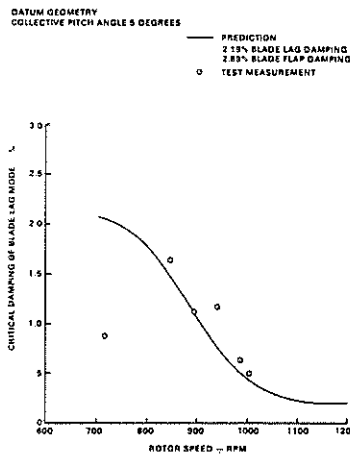


FIGURE 10

## 7.2 Nine Degrees Collective Pitch Case with Negative Pitch-Lag Coupling

Negative pitch-lag coupling (as defined by CL70) was obtained by inclining the control rod at 15 deg. to the vertical. The top of the rod was radially inboard of the bottom of the rod, with respect to rotor radius.

The stability predictions and measured points are shown in Figure 9. The theoretical predictions show an increase in stability compared with the datum case with vertical track rod, of approximately 0.5% of critical, over the range tested. The measured values are quite consistent with predictions, most values lying within 0.5% of the theoretical curve. There is some scatter, although fewer measurements were made than for the previous case.

## 7.3 Five Degrees Collective Pitch Case

Figure 10 shows results for this case presented in the same form as Figure 8. Clearly the trend in prediction is a small increase in stability margin over the 9 deg. (vertical track rod) case. Comments about the accuracy of measurements can be made as for the previous cases. Few measured values were obtained at this condition, and all but the 720 rpm value lie close to the predicted curve.

## 8. AIR RESONANCE RESULTS

### 8.1 Quality of Data

The data obtained from the air resonance rig was, in general, characterised by a clarity in the blade lag response to the initial disturbance which allowed a great degree of confidence to be placed in the validity and repeatability of the estimated damping levels derived from applications of the Moving Block. Figure 11 includes an example lag signal from the air resonance rotor, in which the clarity of response is evident. Note can also be made in this Figure of the associated clear responses of the fuselage in pitch and roll.

This improvement over the data from the ground resonance rig could be recognised as being a result of lower levels of background signal, mostly at once-per-rev., and a higher magnitude of initial disturbance generated by application of cyclic pitch to the rotor. The lower once-per-rev. content suggested a greater symmetry in this rotor or beneficial effects of differences in rig mounting, including wake effects, compared with the ground resonance rig.

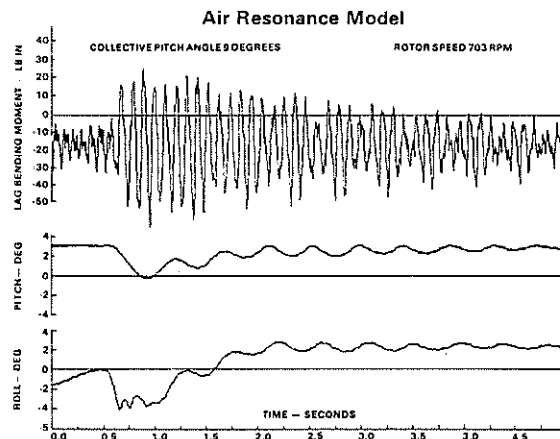


FIGURE 11

FIGURE 12

Air Resonance Model  
Predicted and Measured Stability Margins

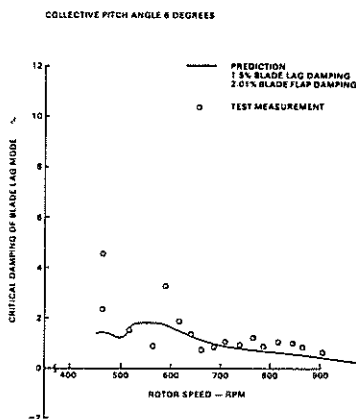
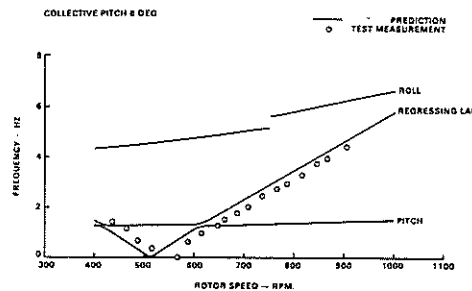


FIGURE 13

Air Resonance Model  
Variation of Mode Frequency with Rotor Speed



## 8.2 Six Degrees Collective Pitch Case

The results for blade lag stability margin are given in Figure 12. There is good agreement between the predicted line and measured points, but with some scatter of measurements in the 450 to 600 rpm range.

Figure 13 shows corresponding predicted mode frequencies and measured lag mode frequencies, expressed in a non-rotating frame of reference. Two predicted modes attributed to fuselage motion are designated "roll" for the higher frequency and "pitch" for the lower frequency. Since the pitch and roll frequencies due to structural stiffness of the rig are very low, deriving from the stiffness of the flexible joint in the rotor drive system, the final values of these frequencies are dependent on coupling with rotor flapping, in the recognised air resonance manner.

It can be seen that in the region 450 to 600 rpm the regressing lag mode frequency approaches zero and then increases again. The blade lag frequency (in the rotating frame of reference) hence approaches once-per-rev. in this region, making accurate measurement of damping by the Moving Block technique more difficult. The rotor becomes least stable as the regressing lag mode approaches the roll mode at high rotor speeds. There is no clear minimum in stability caused by coalescence of pitch and regressing lag modes.

A difference of around 0.4Hz in predicted lag frequency, compared with measurement, is apparent. This is similar to that seen on the ground resonance rotor.

## 8.3 Nine Degrees Collective Pitch Case

For the limited number of test points obtained at this setting, good agreement is shown between prediction and measurement in Figure 14, to within 0.5% of critical damping, apart from some scattered points with high damping levels between 400 and 500 rpm which are probably associated with the once-per-rev. response rather than the blade lag decay. The minimum stability was seen around 650 rpm due to coalescence of the pitch mode with the regressing lag mode.

## 8.4 Twelve Degrees Collective Pitch Case

Figure 15 shows measured stability points for this case, together with theoretical predictions plotted as the solid line. Agreement between measurement and prediction is good in the overall form of the graph up to 875 rpm and predictions are close to measurement at 450 rpm and in the range 650 to 900 rpm. There is an apparent shift between prediction and measurement of the minimum stability speed at coalescence of pitch and regressing lag modes.

Additional measured points above 900 rpm were obtained for this case, at the limit of expected hub flexure element strength. The values show a clear decrease in stability, while predictions indicate a very shallow reduction. Only limited running of the rotor was possible at this high speed range, as a complete structural failure of the hub was sustained. The discrepancy between theory and measurement may have been a result of a radical change in flexure element characteristics just prior to the failure, but this supposition could not be substantiated.

Air Resonance Model  
Predicted and Measured Stability Margins

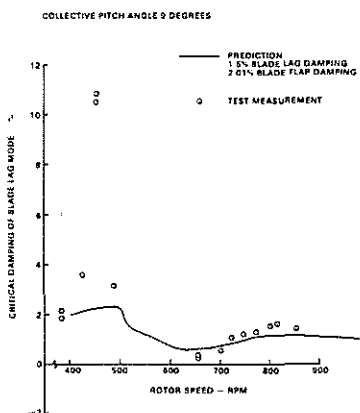


FIGURE 14

Air Resonance Model  
Predicted and Measured Stability Margins

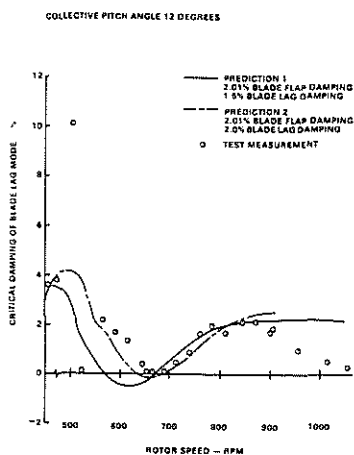


FIGURE 15

Air Resonance Model  
Variation of Mode Frequency with Rotor Speed

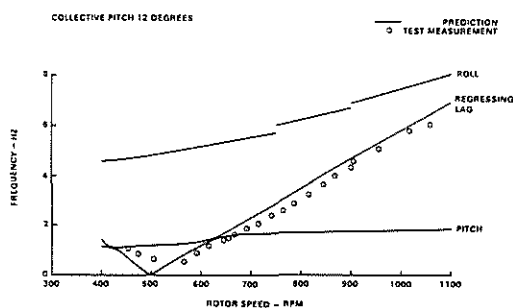


FIGURE 16

Air Resonance Model - Predicted  
Stability for Constant Values of Pitch/Lag  
Coupling CL70

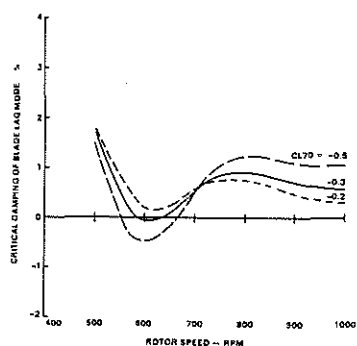


FIGURE 17

The dashed line on Figure 15 is a theoretical prediction arrived at after a parametric study in the analytical method. The excellent agreement (up to 900 rpm) was achieved by setting the blade lag mode frequency used in the computer program to the measured value of 10.6Hz at 900 rpm (instead of 10.2Hz) and increasing blade lag mode inherent damping from 1.5% to 2.0% of critical. Adjustment of the lag mode frequency at 600 rpm, also used in the computer program, was made to give the same derived structural stiffness value as that found for the 10.6Hz frequency at 900 rpm, on the basis that the actual measured frequency at 600 rpm would be influenced by the pitch mode proximity (Figure 16). These changes in frequency and damping required for the "best-fit" prediction are comparatively small.

### 8.5 Effect of Pitch-Lag Coupling

The pitch-lag couplings for the air resonance cases discussed above range from  $CL70=0.119$  at 6 deg. collective to  $CL70=-0.580$  at 12 deg. collective, at 900 rpm. Disregarding the measured points above 900 rpm for the 12 deg. collective case, the trend in air resonance stability for these cases is for stability margins associated with the fuselage "pitch" mode to decrease and

that associated with the "roll" mode to increase with increasingly negative pitch-lag coupling. However, the primary effect of collective pitch on stability is also present.

In order to further investigate this trend, a parametric study using the predictive analysis was undertaken, using different values of pitch-lag coupling at constant collective pitch and assuming a low value of pitch-flap coupling. The results, plotted in Figure 17, confirmed the observed trend noted above.

## 9. GENERAL DISCUSSION

### 9.1 Comparison of Prediction and Measurement

There has been generally good agreement between prediction and measurement for ground and air resonance in this study. The quality of measured data from the ground resonance rig was not as high as that obtained from the air resonance rig. Reasons for this have been identified as differences in methods of excitation and possible rotor asymmetry in particular. Rotor symmetry, inherent damping, allowable levels of excitation, allowable speed range and life were limited by the constraints associated with the material and configuration used for the hub flexure elements.

The stability analysis has proved adequate as a predictive tool for a bearingless rotor, although full use of the coupled blade modes would seem a more thorough approach. An analysis under development by Patel and Done at City University, London, (Reference 7) uses automatic generation of equations of motion for theoretical prediction of helicopter stability, from fully coupled blade modes. The test results reported here will provide data for substantiation of this analysis.

### 9.2 Torque-tube Damper Model

The damper model described in Section 3.1 was originally envisaged as a means of representing a full-scale scheme for adding damping by incorporating elastomer material to restrain changes in torque-tube length resulting from lead-lag motion. High levels of damping encountered in implementing this scheme at model scale made measurement of stability margins very difficult. An alternative method of testing for ground resonance stability of this configuration was evaluated by shaking the fuselage in roll over a swept range of frequency and measuring the receptance (displacement/force) at the shaker input, with the rotor running at constant speed. This was found to be unsatisfactory at the levels of damping present, failing to detect the rotor lag mode response.

### 9.3 Implications for a Full-Size Rotor

The model rotor was not a precise representation of a proposed full-scale rotor, but was rather a means of substantiating the analyses with results which are in a relevant area because of dynamic similarity of important rig parameters to full-size.

Of particular interest are the values of pitch lag coupling seen in the bearingless rotor configuration, which are known to affect stability. For the ground resonance rotor, with datum vertical track rod, magnitude of pitch-lag coupling is low compared with that predicted for a full-scale rotor design scheme. This difference can be attributed to dissimilar relative blade stiffness and lift distributions. However, inclination of the track rod enabled high negative values to be induced. For the air resonance rotor the lower control circuit stiffness results in a range of pitch-lag coupling (from positive at low thrust to highly negative at high thrust) similar to that predicted at full-scale (with an accompanying high level of pitch-flap coupling not seen in full scale schemes).

If the results for the model are considered as if they were for a full-size main rotor, certain observations can be made. In ground resonance, measurements show the rotor to be stable up to 1000 rpm, while predictions show the rotor unstable by a very small margin above 1000 rpm at 9 deg. collective pitch (without negative pitch-lag coupling). The scaled normal operating speed is 900 rpm. Mean inherent lag damping of 2.19 % was measured for the rotor, and used in the calculations. Inherent damping levels for a full-size hub may be lower, due to use of higher volume-fraction materials and the effect of scale on sliding components, perhaps as low as 0.5 % . It can therefore be concluded that added damping would be required to ensure stability. Proposals for a full-scale hub suggested added damping of 3 % of critical. Results from these tests are consistent with that recommendation. Not considered in this discussion is the possible destabilising effect of higher thrust levels than tested, or the stabilising effect of added fuselage damping. In Reference 8 , added structural damping was identified as the most powerful method of ensuring stability margins for a bearingless main rotor.

The air resonance results (measured and predicted) show the rotor to be at worst neutrally stable in the range 80 % to 120 % of normal operating speed (700 to 1100 rpm). With the mean measured inherent lag damping level of 1.50 % of critical, it can again be seen that a full-scale rotor would require added damping in order to provide a margin of stability. A damper providing 2 % of critical damping might be expected therefore to give a stability margin in the conditions tested of approximately 1.0 % . If the results in Figure 15 are considered, it can be seen that although it is important to explain the large difference between measurement and prediction at high rotor speeds, in this case the minimum measured stability margin in the speed range of interest is not reduced by the high speed values, due to the presence of the minimum at lower speeds.

A potentially important case at low thrust (the nearest test condition to autorotation) is shown in Figure 12. Here the effect of positive pitch-lag coupling and of low coning is such that the stability curve is flattened at lower speeds and the approach of instability at high speeds is of most importance.

The test conditions have been limited to the hover. Previous semi-rigid rotor configurations have been predicted to exhibit minimum air resonance stability in the hover, and a trend of increasing stability with forward speed is reported in Reference 9. Predicted results for a full scale scheme have suggested that this may not always be true for a bearingless rotor.

## 10. CONCLUSIONS

The aim of the investigation, to provide substantiation of predictive analysis for ground and air resonance of a bearingless rotor, has been achieved, with generally good agreement between measured and theoretical data, particularly for the air resonance cases.

The Moving Block technique has proved effective in measurement of stability margins. In using this technique, the importance has been demonstrated of adequate levels of initial excitation, rotor symmetry and separation of lag oscillation from the once-per-rev. frequency.

Measurement and prediction suggest that the rotor is at worst marginally unstable in ground resonance (at high rotor speed) and neutrally stable in air resonance.

Increasing negative pitch-lag coupling is shown to have a stabilising effect on the ground resonance case and on the fuselage roll mode in air resonance, while reducing stability of the fuselage pitch mode in air resonance.

The stability margins in ground and air resonance, allowing for the inherent damping of the model rotor hub, are consistent with a requirement for added damping of 3 % of critical in a full-scale main rotor.

## 11. REFERENCES

1. D.H.Hodges, E.H.Dowell      Nonlinear Equations of Motion for the Elastic Bending and Torsion of Twisted Nonuniform Rotor Blades.  
NASA Report TN D-7818 1974
2. P.G.C.Dixon                      Design, Development and Flight Demonstration of the Loads and Stability Characteristics of a Bearingless Main Rotor.  
USAAVRADCOM-TR-80-D-3 1980
3. S.P.King                              Helicopter Ground Resonance Experimental Validation of Theoretical Results by the Use of a Scale Model.  
8th European Rotorcraft Forum 1982
4. S.P.King                              Theoretical and Experimental Investigations into Helicopter Air Resonance.  
39th Annual Forum of the American Helicopter Society 1983

5. W.G.Bousman, D.J.Winkler      Application of the Moving Block  
Analysis.  
USAAVRADCOM 81-0653
6. M.J.McNulty                      Effects of Blade to Blade  
Dissimilarities on Rotor-Body  
Lead-Lag Dynamics.  
11th European Rotorcraft Forum  
1985
7. M.H.Patel, G.T.S.Done          Experience with a New Approach to  
Rotor Aeroelasticity.  
10th European Rotorcraft Forum  
1984 and Vertica 9,(3), 1985
8. W.H.Weller, R.L.Peterson      Inplane Stability Characteristics  
for an Advanced Bearingless Main  
Rotor Model.  
39th Annual Forum of the American  
Helicopter Society 1983
9. V.Kloppel, K.Kampa,  
B.Isselhorst                      Aeromechanical Aspects in the  
Design of Hingeless/Bearingless  
Rotor Systems.  
9th European Rotorcraft Forum  
1983

#### Acknowledgements

The author would like to express his thanks to Mr J.W.Higgs of EEL Limited for his work in the design, build and test of the model rotor.

The investigation was partly funded by the Ministry of Defence Procurement Executive.